Development 129, 5323-5337

doi:10.1242/dev.00100

Shh signaling within the dental epithelium is necessary for cell proliferation, growth and polarization

Amel Gritli-Linde[1,*], Marianna Bei[2], Richard Maas[2], Xiaoyan M. Zhang[3], Anders Linde[1] and Andrew P. McMahon[4,*]

[1]Department of Oral Biochemistry, Sahlgrenska Academy at Göteborg University, SE-405 30 Göteborg, Sweden
[2]Division of Genetics, Brigham and Women's Hospital, Harvard Medical School, 20 Shattuck Street, Boston, MA 02115, USA
[3]Curis Inc., 45 Moulton Street, Cambridge, MA 02138, USA
[4]Department of Molecular and Cellular Biology, Harvard University, 16 Divinity Avenue, Cambridge, MA 02135, USA
*Authors for correspondence (e-mail: amcmahon@mcb.harvard.edu and amel@odontologi.gu.se)

Accepted 12 August 2002

SUMMARY

***Sonic hedgehog* (*Shh*), a member of the mammalian Hedgehog (Hh) family, plays a key role during embryogenesis and organogenesis. Tooth development, odontogenesis, is governed by sequential and reciprocal epithelial-mesenchymal interactions. Genetic removal of Shh activity from the dental epithelium, the sole source of Shh during tooth development, alters tooth growth and cytological organization within both the dental epithelium and mesenchyme of the tooth. In this model it is not clear which aspects of the phenotype are the result of the direct action of Shh on a target tissue and which are indirect effects due to deficiencies in reciprocal signalings between the epithelial and mesenchymal components. To distinguish between these two alternatives and extend our understanding of Shh's actions in odontogenesis, we have used the *Cre-loxP* system to remove Smoothened (Smo) activity in the dental epithelium. Smo, a seven-pass membrane protein is essential for the transduction of all Hh signals. Hence, removal of Smo activity from the dental epithelium should block Shh signaling within dental epithelial derivatives while preserving normal mesenchymal signaling. Here we show that Shh-dependent interactions occur within the dental epithelium itself. The dental mesenchyme develops normally up until birth. In contrast, dental epithelial derivatives show altered proliferation, growth, differentiation and polarization. Our approach uncovers roles for Shh in controlling epithelial cell size, organelle development and polarization. Furthermore, we provide evidence that Shh signaling between ameloblasts and the overlying stratum intermedium may involve subcellular localization of *Patched 2* and *Gli1* mRNAs, both of which are targets of Shh signaling in these cells.**

Key words: Sonic hedgehog, Smoothened, Patched2, mRNA subcellular localization, CyclinD1, Cell polarity, Cell size, ZO-1, Molar fusion, Tooth, Mouse

INTRODUCTION

The first visible indication of the initiation of odontogenesis is the appearance of a local thickening of the oral ectoderm, which subsequently grows into the underlying neural crest-derived mesenchyme of the first branchial arch to form epithelial buds. Ectomesenchymal cells condense around the epithelial buds to form the dental mesenchyme. The primary enamel knot, a tooth signaling center (Vaahtokari et al., 1996; Jernvall et al., 1998), becomes prominent at the cap stage. At the bell stage, the tooth consists of an epithelial enamel organ (EEO) and a dental mesenchyme. The EEO components include proliferating preameloblasts and their progenitors, the cells of the inner dental epithelium (IDE), the secondary enamel knots at the tip of nascent cusps, the stellate reticulum (SR), the outer dental epithelium (ODE) and the stratum intermedium (SI). The latter consists of squamous cells adjacent to the IDE and preameloblasts. Later-arising secondary enamel knots, which form in the developing molars, are thought to control cuspal morphogenesis and terminal differentiation of odontoblasts (Thesleff et al., 2001). Mesenchymal cells of the dental papilla that lie adjacent to the IDE form the preodontoblast layer of proliferating cells; the rest of the dental papilla cells contribute to the later development of the dental pulp. Finally, dental mesenchyme that surrounds the tooth germ forms the dental sac, which gives rise to periodontal tissues.

During the cytodifferentiation stage, the terminal differentiation of odontoblasts is accomplished by their withdrawal from the cell cycle, elongation, polarization and secretion of a predentin matrix. This, in turn, triggers terminal differentiation of ameloblasts (Slavkin and Bringas, 1976; Frank and Nalbandian, 1989). Differentiation of the ameloblast into a highly-polarized complex secretory cell involves considerable growth, elongation of the cytoplasm, a change in nuclear polarity, a sequential development and change in

polarity of organelles, and the appearance of a complex cytoskeleton (Slavkin, 1974). During this stage, there are other progressive changes within the enamel organ. Cells from the SI that are adjacent to polarizing post-mitotic ameloblasts become cuboidal in shape, except in the future enamel-free areas in rodent molars (Cohn, 1957; Gaunt, 1956; Hay, 1961). In addition, the SR is invaded by blood vessels and fibroblasts emanating from the dental sac (Lefkowitz et al., 1953; Hay, 1961).

The rodent incisor is unique in its tissue organization and consists of stem cells, differentiating cells and mature cells organized in defined regions along its anteroposterior and labial-lingual axes. The rodent incisor is asymmetrical, as the labial or amelogenic IDE gives rise to ameloblasts and enamel, whereas the IDE on the lingual side does not produce enamel. The posterior-most aspect of the incisor has been postulated to contain stem cells which give rise to the different dental cell populations (Smith and Warshawsky, 1975; Harada et al., 1999). A posteroanterior gradient of cytodifferentiation is thus present in the rodent incisor throughout life, with the less differentiated cells located posteriorly and the most mature cells anteriorly. Odontoblasts differentiate all along the epitheliomesenchymal interface of the incisor (Cohn, 1957; Warshavsky, 1968).

Like many organs, morphogenesis and cytodifferentiation of the tooth is governed by sequential and reciprocal epithelial-mesenchymal interactions mediated by several soluble bioactive proteins (Jernvall and Thesleff, 2000; Thesleff et al., 2001; Thesleff and Mikkola, 2002). In addition, cell-matrix interactions and cell-cell junctional complexes and cytoskeletal components have been implicated in the regulation of histomorphogenesis and proliferation (Thesleff et al., 1981; Lesot et al., 1982; Fausser et al., 1998).

Sonic hedgehog (*Shh*), a member of the vertebrate Hedgehog (Hh) family, encodes a secreted signaling peptide. Hedgehog signals are received within a target tissue by the general Hedgehog receptor Patched 1 (Ptc1 in mammals; *Ptch* – Mouse Genome Informatics) [for review of pathway see Ingham and McMahon (Ingham and McMahon, 2001)]. Transduction of the signal within a responding cell absolutely requires the activity of a second, multi-pass, membrane protein Smoothened (Smo). Smoothened activity leads to a conserved transcriptional response: up-regulation of *Ptc1* and *Gli1* in the target tissue. *Gli1* encodes a member of the Ci/Gli family of transcriptional effectors of Hedgehog signaling.

The Hh signaling pathway is an evolutionarily well-conserved mechanism involved in a plethora of biological processes (for reviews, see Ingham and McMahon, 2001; McMahon et al., 2002). *Shh* is expressed exclusively in the epithelial component of the murine tooth from the dental lamina stage until cytodifferentiation (Bitgood and McMahon, 1995; Vaahtokari et al., 1996; Hardcastle et al., 1998; Dassule et al., 2000; Gritli-Linde et al., 2001). At the cap stage, *Shh* is confined to the primary enamel knot (Vaahtokari et al., 1996; Hardcastle et al., 1998). Expression spreads thereafter to the rest of the IDE laterally, the stratum intermedium (Dassule et al., 2000; Gritli-Linde et al., 2001) and the stellate reticulum (Gritli-Linde et al., 2001). At the cap stage, general transcriptional targets and effectors of Shh signaling, including *Ptc1*, *Gli1* and *Smoothened* (*Smo*) are, however, expressed in both dental epithelium and mesenchyme, but are excluded from the enamel knot (Hardcastle et al., 1998). In contrast, Ptc2, while appearing to bind all mammalian Hedgehog proteins similarly to the related Hedgehog receptor Ptc1 (Carpenter et al., 1998), is expressed in the enamel knot and IDE at the cap and early bell stages, respectively (Motoyama et al., 1998).

We have shown previously that Shh protein produced by the enamel knot and IDE moves many cell diameters to reach the rest of the dental epithelium and the dental papilla, indicating that Shh has a long-range activity, consistent with the broad expression of *Shh* target genes (Gritli-Linde et al., 2001). Together, the above observations suggest that Shh signaling may be operative intra-epithelially as well as in mediating epithelial-mesenchymal interactions during tooth development. Finally, we have shown that genetic removal of Shh activity from the tooth leads to alterations in growth and morphogenesis and results in tissue disorganization, affecting both the dental epithelium and mesenchyme derivatives (Dassule et al., 2000). In this study, it was not possible to determine clearly whether the alterations in the dental mesenchyme and its derivatives were solely generated by lack of Shh signaling by the dental epithelium, or whether they were secondary to the lack of proper signaling – via other bioactive molecules – in the abnormal dental epithelium. Conversely, this approach left unanswered the question of whether abnormal development of the epithelial enamel organ in *Shh* mutant teeth was a result of a loss of intra-epithelial Shh signaling, or a secondary consequence of altered signaling by the underlying dysplastic dental mesenchyme.In order to distinguish between these alternatives, and further define the roles of Shh in regulating morphogenesis of the tooth, we abrogated Shh signal transduction by genetically removing the activity of Smo from the dental epithelium and its derivatives while maintaining Shh responsiveness in the dental mesenchyme.

MATERIALS AND METHODS

Generation of *Smo* conditional mouse lines

The *Smo* conditional allele (Smo^c) and the *Smo* null allele (Smo^n) were generated as described (Zhang et al., 2001; Long et al., 2001). To remove Smo activity from the dental epithelium, we used mice expressing Cre recombinase under the regulation of the enhancer element of *cytokeratin 14* (*K14*) (Dassule et al., 2000). Mice expressing the highest levels of *Cre* RNA in the skin were crossed to a *Smo* null allele (Zhang et al., 2001) to generate mice that were heterozygous for both the *K14-Cre* transgene and a Smo^n allele (*K14-Cre;* $Smo^{+/n}$). Mutant embryos were produced by crossing the *K14-Cre;* $Smo^{+/n}$ mice to $Smo^{c/c}$ mice. Embryos and new-borns were genotyped by PCR as described previously (Zhang et al., 2001; Long et al., 2001). The generation of mice lacking Shh activity in the dental epithelium was as described previously (Dassule et al., 2000).

Electron microscopy and histology

The tips of the mandibles containing the lower incisors from control and mutant pups at 1 day post-partum (1 dpp) were processed for transmission electron microscopy (TEM) as described previously (Sun et al., 1998). Sections for histology were prepared according to routine procedures and stained with Hematoxylin and Eosin.

In situ hybridization

Sections from embryos and 1 dpp pups were prepared for in situ hybridization with ^{35}S-UTP-labeled riboprobes essentially as described previously (Wilkinson et al., 1987). The following probes

were used: *Bmp2*, *Bmp4* and *Bmp7* (Åberg et al., 1997); PDGFRα (Boström et al., 1996); *amelin* (Cerny et al., 1996; Fong et al., 1998); *Shh*, *Ptc2*, *Gli1*, *Gli2*, *Gli3*, *Dentin Sialoprotein* (*DSP*), *Dentin Matrix Protein 1* (*DMP1*) and *Msx2* (Dassule et al., 2000); *cyclin D1* (Long et al., 2001); *Dlx3* and *Dlx7* (Zhao et al., 2000); *Ptc1* (Gritli-Linde et al., 2001). A 1 kb *Bmp5* pro-region fragment was also used to generate an anstisense RNA probe.

Immunohistochemistry and von Kossa staining

Tissues were fixed in either 4% paraformaldehyde in 0.1 M phosphate buffer, pH 7.4, or in Sainte Marie's solution, embedded in paraffin and processed for immunohistochemistry as described previously (Gritli-Linde et al., 2001). The following antibodies were used: rabbit anti-amelin (Fong et al., 1998); rabbit anti-phospho-histone H3 (Ser 10) (Cell Signaling Technology); Ab80 anti-SHH (Bumcrot et al., 1995; Marti et al., 1995); rabbit anti-calbindin-D28K (Chemicon); rat anti-E-cadherin and rabbit anti-ZO1 (Zymed Laboratories); rabbit anti-collagen type IV (ICN Pharmaceuticals); mouse monoclonal anti-β-tubulin clone 5H1, IgM fraction (BD Pharmingen).

For staining of mineralized extracellular matrix, we used a modified method based on the von Kossa technique (Stevens et al., 1990).

RESULTS

Removal of Smo activity from the dental epithelium

We have previously described a *K14-Cre* transgene that is active specifically within the dental epithelium and its derivatives from shortly after the initiation of tooth development (Dassule et al., 2000) and a *Smo* conditional allele (*Smo*^{c}) which allows the Cre-dependent removal of Shh responsiveness in a target cell (Long et al., 2001). In the developing tooth, *K14* is expressed in all components of the epithelial enamel organ (EEO) (Tabata et al., 1996; Dassule et al., 2000). We have previously shown (Dassule et al., 2000) efficient Cre activity in the skin and oral ectoderm, including the dental lamina at 11.75 days post-coitum (dpc), and throughout the dental epithelium by 14.5 dpc.

To create a dental epithelium devoid of Smo activity, we crossed *K14-Cre; Smo*$^{+/n}$ males to *Smo*$^{c/c}$ females. As expected, approximatively 25% of newborns were the experimental genotype (*K14-Cre; Smo*^{c}*/Smo*^{n}), hereafter referred to as 'Smo mutants' for simplicity. All mutant pups were of a normal size and displayed normal external features but died within one day of birth for unknown reasons. Throughout, we compare development of teeth from *K14-Cre;Smo*^{c}*/Smo*^{n} to those of *Smo* heterozygotes (*Smo*^{c}*/Smo*^{n}), hereafter referred to as 'controls'. *Smo*^{c}*/Smo*^{n} embryos and pups were phenotypically similar to wild-type animals.

Smo ablation in the dental epithelium generates cytological alterations within the enamel organ and disrupts normal morphogenesis of the tooth

In order to determine the outcome of *Smo* ablation from the dental epithelium, we analysed histological sections from maxillae and mandibles at 1 day post partum (dpp). As in wild-type pups, incisors and molars developed in both jaws of *Smo* mutants. Ablation of Shh activity within the tooth generates abnormally small and misshapen teeth (Dassule et al., 2000). In contrast, general growth of molars in *Smo* mutants was essentially similar to that of control littermates (Fig. 1A-D). Primary and secondary enamel knots developed normally in *Smo* mutant molars and expressed appropriate specific molecular markers, such as *Bmp2*, *Bmp4*, *Shh*, *Ptc2* and *Msx2* (see below and data not shown). Despite their normal growth, *Smo* mutant molars exhibited several morphological abberrations. Parasagittal sections at 1 dpp revealed that the first and second molars, in both the maxilla and mandible, were abnormally fused, forming a single gigantic anlage (Fig. 1A,B). The molars also fuse in *Shh* mutants; however, the single anlage in those mice were much smaller than those of *Smo* mutant mice (data not shown). On parasagittal and frontal sections, the 'first molars' of *Smo* mutant pups displayed shallow, broad, underdeveloped and misshapen cusps as compared to controls (Fig. 1A-D). As in *Shh* mutants (Dassule et al., 2000), *Smo* mutant molars developed close to the oral surface, reflecting the virtual absence of a dental cord (Fig. 1C,D). However, in contrast to *Shh* mutants (Dassule et al., 2000), at all developmental stages the mesenchyme of the *Smo* mutant molars appeared to have normal cellularity, temporospatial patterns of odontoblast terminal differentiation and secretion of a predentin matrix (Fig. 1C,D).

The principal cytological differences were observed in the dental epithelium derivatives. A disorganization within the EEO was evident at the late bell stage in the principal cusps of the 'first molars'. In the less-developed cusps of the 'first and second molars', the EEO cytological organization was normal, similar to that of controls (Fig. 1A,B). At the tip of the principal cusps of late bell stage first molars from control 1 dpp pups, elongated polarizing, post-mitotic ameloblasts lay adjacent to a predentin matrix. The ameloblast were overlaid by the SI, which had assumed a cuboidal shape. The ODE developed into a discontinuous layer, and the coronal aspect of the SR displayed the normal metaplastic changes secondary to the initiation of its invasion by early vascular loops and fibroblasts that emanate from the dental sac, through gaps in the ODE (Fig. 1C). In the most advanced cusps of the first molar region of *Smo* mutant, ameloblasts were abnormally short and were overlaid by a scarce, squamous SI. The SR was also hypocellular and did not display the changes characteristic of the process of metaplasia. The absence of early vascular loops in the coronal aspect of the SR was verified by staining of blood vessel basement membrane with an anti-collagen type IV antibody (data not shown). Finally, the mutant ODE formed a continuous layer without the gaps observed in controls (Fig. 1D).

Similar cytological changes were observed, specifically on the labial side of the epithelium of *Smo* mutant incisors. They were, however, more dramatic, as the incisor is developmentally more advanced than the molar. At 1 dpp incisors from control pups contained, on their labial side, enamel matrix secreted by highly polarized secretory ameloblasts overlaid by cuboidal SI cells (Fig. 1E). At this stage, the ameloblasts of mutant incisors had failed to undergo polarized growth and formed a non-cohesive layer of non-polarized cuboidal cells with centrally located nuclei; the enamel matrix was absent (Fig. 1F). The SI overlying ameloblasts was sparse and exhibited a squamous morphology (Fig. 1F). In contrast to molars, the mutant incisors had a smaller diameter than the controls, which was first evident at the differentiation stage. This may reflect the differences between development of molars and incisors in rodents. In addition, the *Smo* mutant incisors exhibited abnormal foldings

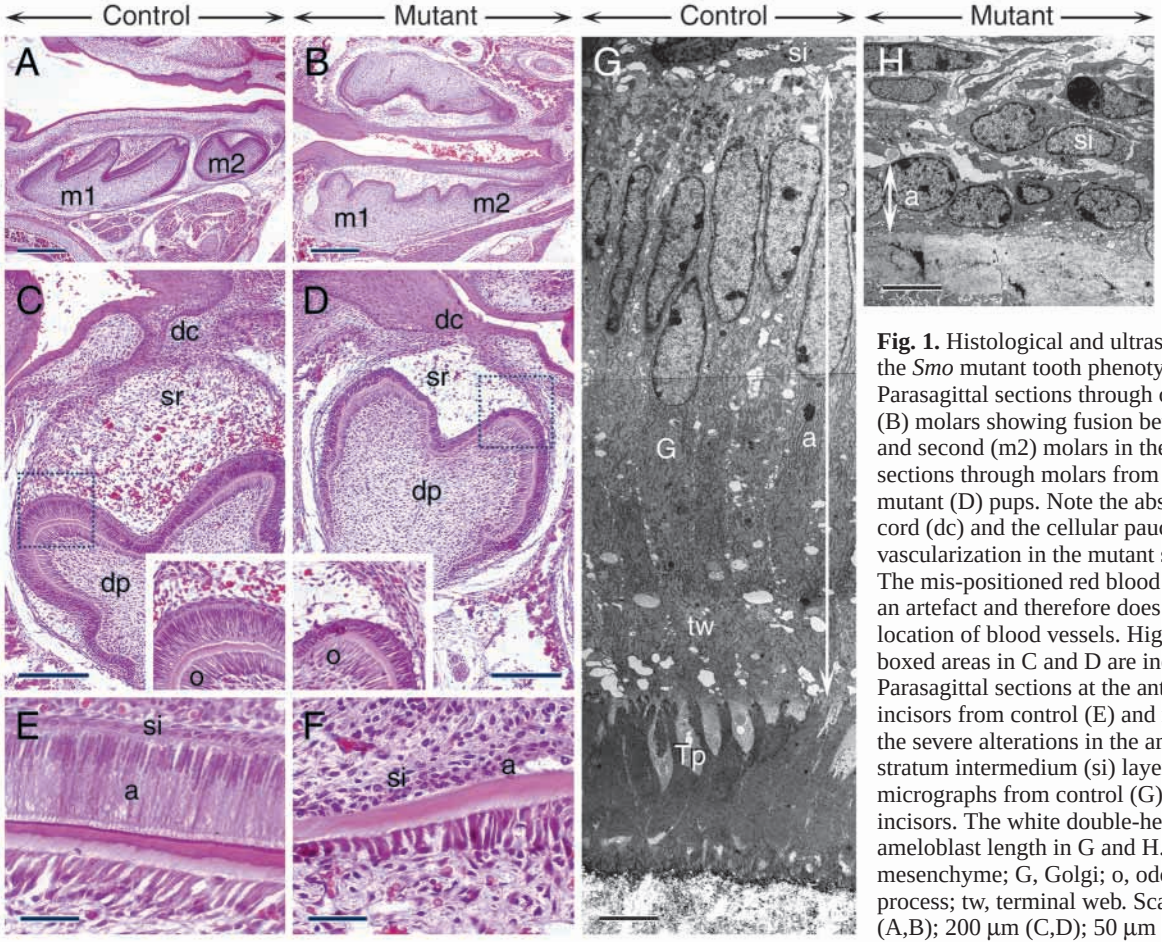

Fig. 1. Histological and ultrastructural analysis of the *Smo* mutant tooth phenotype at 1 dpp. Parasagittal sections through control (A) and mutant (B) molars showing fusion between the first (m1) and second (m2) molars in the mutant. Frontal sections through molars from control (C) and mutant (D) pups. Note the absence of the dental cord (dc) and the cellular paucity and lack of vascularization in the mutant stellate reticulum (sr). The mis-positioned red blood cells in the SR in C is an artefact and therefore does not indicate the exact location of blood vessels. High magnifications of boxed areas in C and D are included as insets. Parasagittal sections at the anterior segment of incisors from control (E) and mutant (F) pups. Note the severe alterations in the ameloblast (a) and stratum intermedium (si) layers in the mutant. TEM micrographs from control (G) and mutant (H) incisors. The white double-headed arrows indicate ameloblast length in G and H. dp, dental papilla mesenchyme; G, Golgi; o, odontoblasts; Tp, Tomes' process; tw, terminal web. Scale bars: 500 μm (A,B); 200 μm (C,D); 50 μm (E,F); 5 μm (G,H).

of the lateral and medial aspects of the IDE at the posterior and middle segments of the tooth, which at certain levels invaginated within the tooth (data not shown). These may also account for the slightly smaller size of the incisor (data not shown). In control incisors, during enamel secretion, a papillary layer consisting of merged SR and ODE was evident, but this structure was absent in the mutant incisors (data not shown).

In order to chararacterize the structural cytological alterations of *Smo* mutant ameloblasts and SI at the subcellular level, we examined and compared their phenotype to that of controls by transmission electron microscopy (TEM) on ultrathin sections taken from incisors at their anterior segment. In control incisors, young secretory ameloblasts were highly columnar, elongated and polarized with oval-shaped nuclei elongated along the apical-basal axis (Fig. 1G). In *Smo* mutant incisors, the cuboidal ameloblasts were only 15% of the apical-basal height of the secretory ameloblasts of control incisors (excluding the Tomes' process) and contained centrally located round nuclei (Fig. 1H). Furthermore, several organelles, including mitochondria, RER and Golgi were both sparse and evenly distributed in the cytoplasm, whereas in controls these organelles were abundant and showed a polarized distribution within the cell. Tomes' processes and the terminal webs had not developed in mutant ameloblasts (Fig. 1H).

Shh regulates cell-cell interactions within the EEO and is essential for development of the cytoskeleton in ameloblasts

Junctional complexes and the cytoskeleton are important in maintaining epithelial cell polarity and cell-cell interactions (Farquar and Palade, 1963; Gundersen and Cook, 1999). To assess whether defects in the EEO in *Smo* mutant teeth were secondary to alterations in the development of these structures, we analyzed by immunohistochemistry the distribution of some markers of these cellular components.

First, we studied the distribution of Zonula Occludens-1 (ZO-1), a member of the membrane-associated guanylate kinase homologues (MAGUKs) and a scaffolding protein associated with tight junctions and other cell-cell contact sites (Tsukita et al., 1999; Vasioukhin and Fuchs, 2001). In control embryos at the early bell stage, ZO-1 staining was abundant in the ODE and less so in the IDE (data not shown). By the late bell stage, in control molars, ZO-1 protein gradually increased at the apicolateral and basolateral domains of polarizing ameloblasts adjacent to the first layer of predentin. At a similar stage, the ameloblasts of mutants showed barely detectable levels of ZO-1 (Fig. 2A-D). The ODE of control molars exhibited reduced ZO-1 immunostaining and formed a discontinuous layer interrupted by gaps penetrated by connective tissue invading the coronal part of the SR (Fig. 2C). In contrast, the ODE of *Smo* mutants remained as a continuous

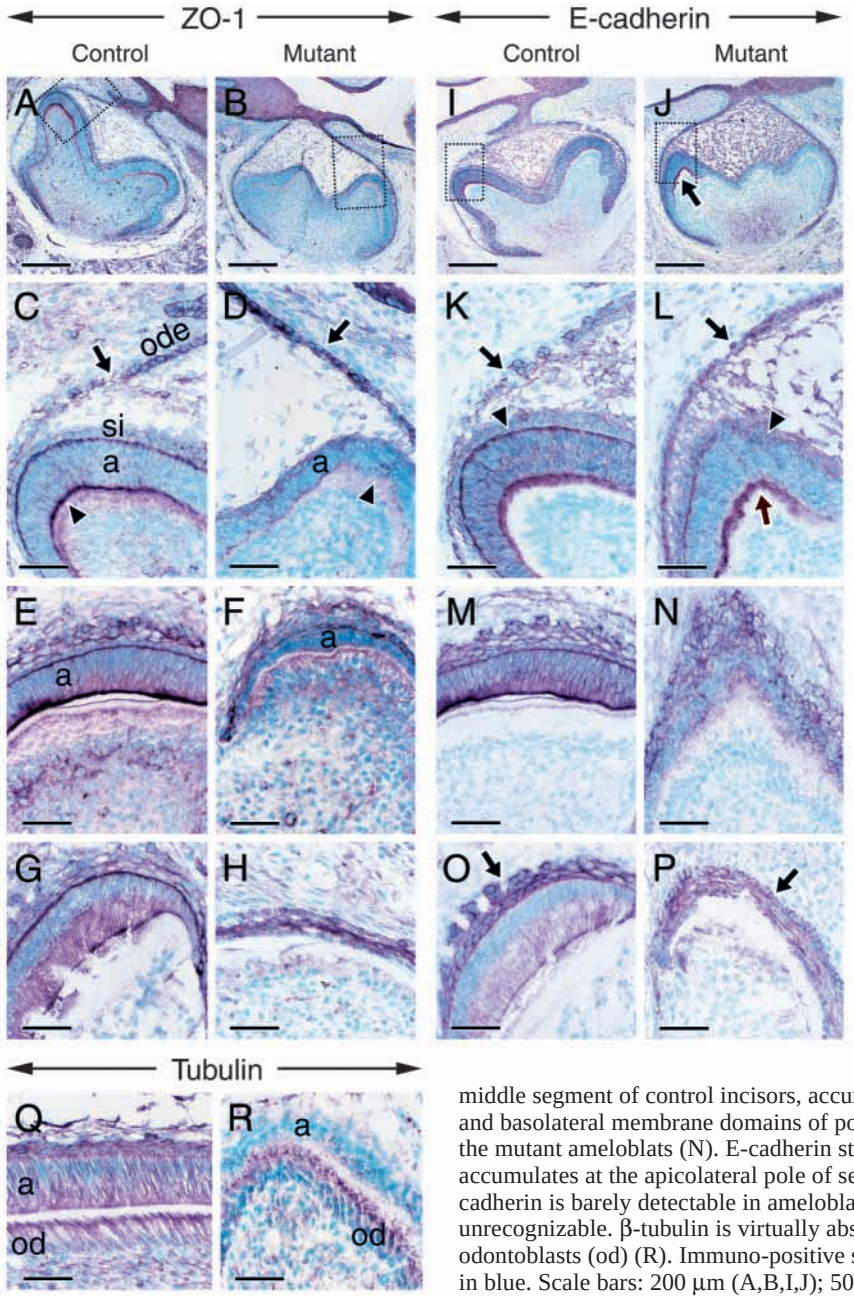

Fig. 2. Immunohistochemical localization of cytoskeletal and junctional complex proteins in *Smo* mutant molars and incisors at 1 dpp. Frontal sections of control (A,C,E,G,I,K,M,O) and *Smo* mutant (B,D,F,H,J,L,N,P) teeth. Parasagittal sections of control (Q) and mutant (R) incisors. ZO-1 (A-H), E-cadherin (I-P) and β-tubulin (Q, R). Sections at the middle segment of incisors (E,F,M,N) and at their anterior-most segment (G,H,O,P). The boxed areas in A and B are shown in C and D, respectively. In the control molars (A,C) and incisors (E), ZO-1 accumulates between polarizing ameloblasts (a) and the stratum intermedium (si) as well as at the apicolateral membrane domain of polarizing ameloblasts (arrowhead in C) facing predentin matrix. The outer dental epithelium (ode) shows gaps (arrow in C) with no ZO-1 staining. At this time, ZO-1 is absent from the apical and basal aspect of *Smo* mutant ameloblasts (a) in molars (arrowhead in D) and incisors (F), whereas it accumulates in the ode (arrow in D), which remains as a continuous layer (B,D). At the anterior-most aspect of the control incisors, ZO-1 accumulation is polarized in the apicolateral and basolateral poles of secretory ameloblasts (G) but is absent in mutant ameloblasts (H). Note that by this stage mutant ameloblasts are severely shrunken, and the strong staining visible is associated with cells of the stratum intermedium and ode (H). E-cadherin staining highlights the gaps in the ode (arrow in K) of control molars (I,K) which are absent (arrow in L) in the mutant molars (J,L). Boxed areas in I and J are shown in K and L, respectively. In some cusps of mutant molars, ameloblasts show some E-cadherin staining at their apicolateral pole (red arrow in L). However, these cells do not show as strong a basolateral E-cadherin accumulation (arrowhead in L) as in controls (arrowhead in K). In the middle segment of control incisors, accumulation of E-cadherin is polarized at the apicolateral and basolateral membrane domains of polarizing ameloblasts (M) but is barely detectable in the mutant ameloblats (N). E-cadherin staining decorates the papillary layer (arrow in O) and accumulates at the apicolateral pole of secretory ameloblasts (O). In mutant incisors, E-cadherin is barely detectable in ameloblasts, and the papillary layer (arrow in P) is unrecognizable. β-tubulin is virtually absent in mutant ameloblasts (a), whereas it is present in odontoblasts (od) (R). Immuno-positive sites are purple and immuno-negative sites are stained in blue. Scale bars: 200 μm (A,B,I,J); 50 μm (C-H,K-R).

layer of cells exhibiting strong ZO-1 staining (Fig. 2D). At more advanced developmental stages, as demonstrated in incisors, *Smo* mutant ameloblasts totally lacked ZO-1 staining, whereas the ODE and SI displayed a strong cytoplasmic accumulation of the protein, in striking contrast to control incisors (Fig. 2E-H).

E-cadherin, the epithelial prototype of the transmembrane core of adherens junctions, which is associated with homotypic cell-cell adhesion, also showed a dynamic distribution in polarizing ameloblasts and ODE of control molars that was similar to that of ZO-1 (Fig. 2I,K). In *Smo* mutant molars, some ameloblasts facing predentin had an apicolateral accumulation of E-cadherin similar to that of control ameloblasts (Fig. 2J,L), but in the less-developed cusps, immunostaining was much weaker in the *Smo* mutant preameloblasts than controls (Fig. 2I,J). Similarly, E-cadherin accumulated at the apicolateral and basolateral membrane domains of polarizing ameloblasts but was weak and disorganized in mutants (Fig. 2M,N). At a more anterior level, E-cadherin staining became strong in cells of the papillary layer (Fig. 2O). In *Smo* mutant incisors, the shrunken ameloblasts showed a weak cytoplasmic staining and the papillary layer was unrecognizable (Fig. 2P).

The polarization of both the ameloblast and odontoblast populations is characterized by the accumulation of microtubules. In control teeth, whereas β-tubulin was present at high levels in functional odontoblasts, in polarizing ameloblasts (Fig. 2Q) and in secretory ameloblasts (data not shown), no such accumulation of β-tubulin protein was detected in *Smo* mutants (Fig. 2R). In contrast, odontoblasts in the mutants displayed normal levels of β-tubulin staining.

Thus, Shh signaling is also necessary for normal development of both the cytoskeletal organization and cell-cell junctional complexes, which are likely to play a role in establishing and maintaining ameloblast polarity and function.

Interestingly, analysis of the expression of *Ptc2* and *Gli1* transcripts indicated that their subcellular distribution was polarized in the developing ameloblasts. *Ptc2* and *Gli1* transcripts were enriched at the basal and perinuclear compartments of polarizing (see Fig. 5K below), presecretory and secretory ameloblasts closest to the *Shh*-expressing SI (Fig. 3A-C and see below). In contrast, transcripts of *Dlx7*, *Bmp7*, *Bmp5* (data not shown), *Gli2* (see below), *Msx2*, *Ptc1* and *Dlx3* (Fig. 3D-F) were either distributed uniformly throughout the ameloblast cytoplasm or enriched at its apical pole. Thus a polarized response to the SI, mediated by Shh signaling could play a role in the Shh-dependent ameloblast polarization that is deficient in *Smo* mutants.

Shh responsiveness is abrogated in the epithelial enamel organ and is conserved in the dental mesenchyme of *Smo* mutant teeth

In order to gain insight into the molecular basis of the cytological alterations within the epithelial enamel organ following removal of Smo activity, we first analysed in detail the expression of *Shh* and its targets and effectors at different developmental stages of tooth development. *Shh* expression and responsiveness in control and mutant molars at the cap stage are represented in the schematics (Fig. 4A,B). At the cap stage, *Shh* was detected in the primary enamel knot in both controls and *Smo* mutants (Fig. 4C,D). *Ptc1* and *Gli1*, primary targets of Shh signaling, were expressed in both the EEO (excluding the enamel knot) and mesenchyme in control teeth (Fig. 4E,G). In contrast, in *Smo* mutants, the EEO exhibited a dramatic loss of *Ptc1* and *Gli1* expressions, whereas the mesenchyme maintained normal expression of both of these genes (Fig. 4F,H). Expression of *Gli2* and *Gli3* (data not shown), *Ptc2* in the enamel knot and *Hip1* (Fig. 4I-L) was similar to controls. These data indicate that, as expected, Shh responsiveness was absent from the EEO but maintained in the dental mesenchyme at the cap stage.

In late bell stage control molars, *Shh* was strongly expressed in the IDE, SR, SI, preameloblasts and differentiating ameloblasts (Fig. 5A). However, in mutant molars, preameloblasts adjacent to either polarized odontoblasts or to predentin, SI and SR showed barely detectable levels of Shh (arrow Fig. 5B). At this developmental stage, *Ptc1* and *Gli1* were expressed in both the EEO and mesenchyme, whereas *Ptc2* expression was confined to the EEO in control molars (Fig. 5C,E,I). In *Smo* mutants, *Ptc1*, *Gli1* and *Ptc2* expressions were severely decreased in the EEO, whereas the mesenchyme showed normal Shh responsiveness (Fig. 5D,F,J). In *Smo* mutant molars, the expression of *Hip1* in the mesenchyme was similar to that of controls (Fig. 5G,H).

Immunohistochemistry for Shh protein showed staining in the EEO and mesenchyme as well as in the basement membrane and predentin matrix in molars from control pups (Fig. 5K). The mutant molars (Fig. 5L) exhibited normal Shh immunostaining in the dental mesenchyme and SR; however, immunostaining was dramatically reduced in preameloblasts adjacent either to polarized odontoblasts or to a thin layer of predentin, as well as in the SI overlying these cells.

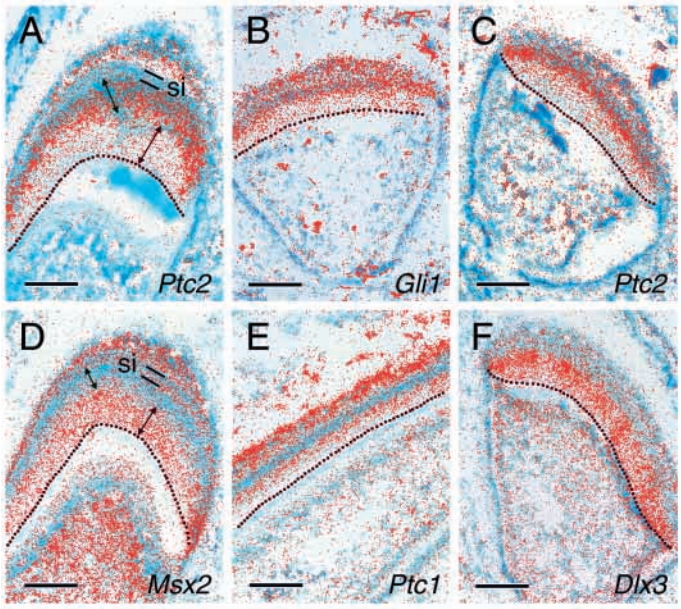

Fig. 3. *Ptc2* and *Gli1* transcripts are polarized in ameloblasts. In situ hybridization on control incisors at 1 dpp at the level of presecretory (A,D) and young secretory ameloblasts (B,C,E,F). Oblique sections (A,D). Frontal sections (B,C,E,F). The dotted lines indicate the ameloblast apical plasma membrane. *Ptc2* (A,C) and *Gli1* (B) mRNAs are enriched at the basal and perinuclear compartment (green arrow) of ameloblasts, causing the signal (red) to mask the blue staining of ameloblast nuclei, whereas the apical pole (red arrow) displays considerably less signal. The extent of the stratum intermedium layer (si) is indicated by bars (A,D). In contrast, mRNAs for *Msx2* (D), *Ptc1* (E) and *Dlx3* (F) are enriched apically (red arrow). Scale bars: 100 μm.

As in molars, alterations of *Shh* expression and responsiveness were also found in the mutant incisors. In the middle segment of control incisors at 1 dpp, *Shh* was strongly expressed in the IDE, SI, preameloblasts and differentiating ameloblasts on the labial side of the tooth (Fig. 5M). In contrast, in *Smo* mutants, *Shh* expression was severely decreased in preameloblasts adjacent either to polarized odontoblasts or to predentin matrix (Fig. 5N). The SI continued to express *Shh* for only a short time before expression was decreased in this cell layer too (Fig. 5N). At this stage, *Ptc1* (data not shown) and *Gli1* (Fig. 5O) were expressed in both the mesenchyme and labial epithelium of control incisors. In contrast, expression of both genes (Fig. 5P and data not shown) was severely decreased in the epithelium but not in the mesenchyme of *Smo* mutant incisors. In the anterior segment of control incisors, *Shh* expression declined in polarizing ameloblasts (arrowhead in Fig. 5Q), dramatically decreased in presecretory ameloblasts (arrow in Fig. 5Q), and was totally abrogated in secretory ameloblasts (data not shown). The SI continued to express *Shh* (Fig. 5Q), even at a more advanced secretory stage (data not shown). In mutant incisors, *Shh* expression was dramatically decreased (Fig. 5R). In control incisors, polarizing, presecretory and young secretory ameloblasts and the SI, expressed *Gli3* (data not shown), *Ptc1*, *Ptc2*, *Gli1* and *Gli2*; however, with the exception of *Gli3* (data not shown), expression of all these genes was decreased to

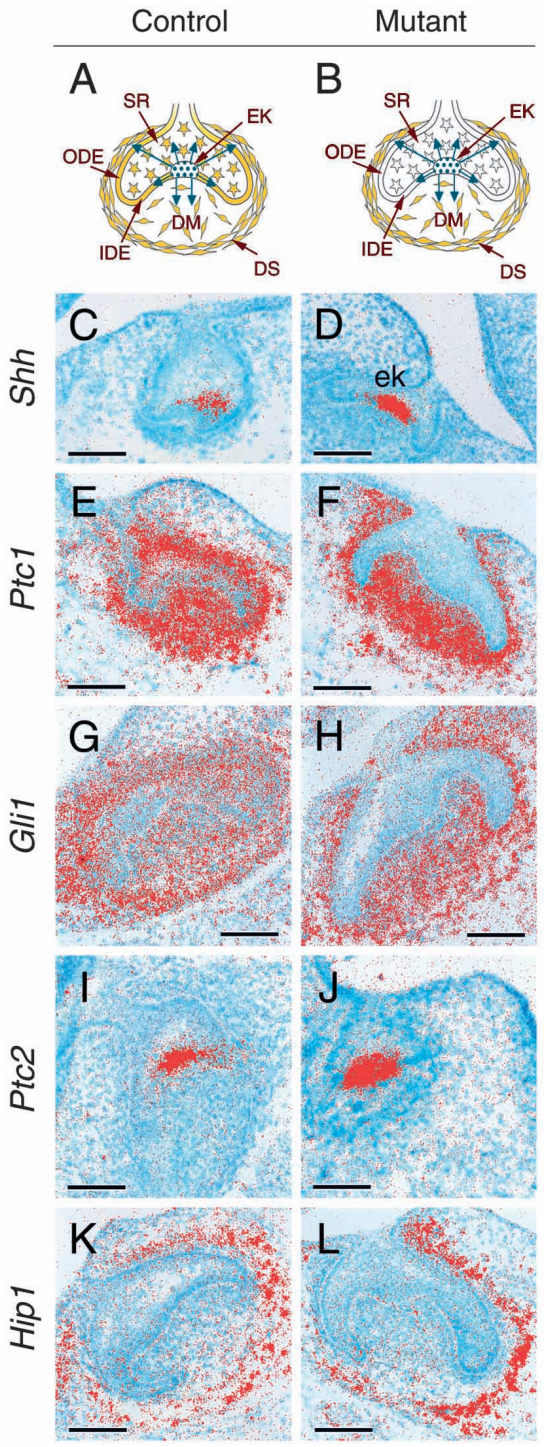

Fig. 4. Analysis of *Shh* expression and Shh responsiveness at the cap stage in *Smo* mutants. Schematic drawings showing tissue organization of molars at the cap stage and *Shh* expression (stippled) and responsiveness (yellow) within the dental epithelium and mesenchyme (A,B). The green arrows show movement of Shh protein. Alterations of Shh responsiveness in the dental epithelium and its preservation in the mesenchyme in *Smo* mutants are summarized in B. In situ hybridizations on frontal sections of molars for *Shh* (C,D); *Ptc1* (E,F); *Gli1* (G,H); *Ptc2* (I,J) and *Hip1* (K,L). DM, dental mesenchyme; DS, dental sac; EK, enamel knot; IDE, inner dental epithelium; ODE, outer dental epithelium; SR, stellate reticulum. Scale bars: 100 μm.

background levels in these cell populations in *Smo* mutants (Fig. 5S-Z).

These data demonstrate that removal of Smo activity from the dental epithelium affects Shh responsiveness within all components of the EEO without altering Shh signaling in the dental mesenchyme. Furthermore, the results provide evidence that in the developing tooth, with the exception of the enamel knot, *Ptc2* transcription is *Shh* dependent, suggesting that *Ptc2*, like *Ptc1*, is a target of Shh signaling, and implicating Ptc2 in the regulation of Shh signaling activity within the EEO.

Shh signaling within the EEO is necessary for regulating cellular proliferation

The *Smo* mutant molars were small, misshapen and had shallow cusps and the incisors were also abnormally small. The enamel knots have been suggested to control cusp morphogenesis in molars. However, primary and secondary enamel knot development in *Smo* mutant molars appeared normal at both the morphological and molecular level. Cell proliferation profiles have been suggested to govern tooth morphogenesis and cytodifferentiation (Ruch, 1990). To address whether cell proliferation, altered by *Smo* loss-of-function, might contribute to the morphological alterations we observed, we first examined the distribution of phosphorylated histone H3 (PH-H3), a marker of mitosis. In control molars and incisors, preameloblasts and the overlying SI facing polarized odontoblasts showed PH-H3 staining. PH-H3 staining was lost thereafter in ameloblasts adjacent to predentin matrix (Fig. 6A and data not shown). In contrast, in *Smo* mutant molars and incisors, PH-H3 staining was lost at an earlier stage, in preameloblasts and SI facing polarized odontoblasts, before predentin secretion (Fig. 6B and data not shown).

Cyclin D1 is a G1 cyclin, which has recently been shown to be transcriptionally induced by Shh and Indian hedgehog (Kenney and Rowitch, 2000; Long et al., 2001). We found that expression of *cyclin D1* was similar in control and *Smo* mutant molars from the cap stage until the early bell stage (data not shown). In the EEO of control molars at 1 dpp, *cyclin D1* was expressed in the IDE, SI and preameloblasts adjacent to polarized odontoblasts. Expression was thereafter abrogated in post-mitotic ameloblasts adjacent to predentin matrix, whereas the SI continued to express *cyclin D1* (Fig. 6C). In *Smo* mutant molars, however, *cyclin D1* transcripts were lost from preameloblasts and the adjacent SI in young cusps that contained polarized odontoblasts but before predentin secretion by these cells (Fig. 6D). As expected, no alterations in PH-H3 staining and *cyclin D1* expression were found in the dental mesenchyme (Fig. 6A-D). Thus, it is likely that mutant preameloblasts and cells of the SI exit the cell cycle prematurely, and that Shh may promote proliferation within the dental epithelium at least in part through the transcriptional regulation of *cyclin D1*.

To assess whether the premature withdrawal from the cell cycle of mutant ameloblasts was associated with their differentiation, we examined the expression of *amelin* and its protein product as well as calbindin D28K immunostaining. These markers are expressed in differentiating and in mature ameloblasts (Elms and Taylor, 1987; Fong et al., 1998). In control molars and incisors, *amelin* mRNA and protein were

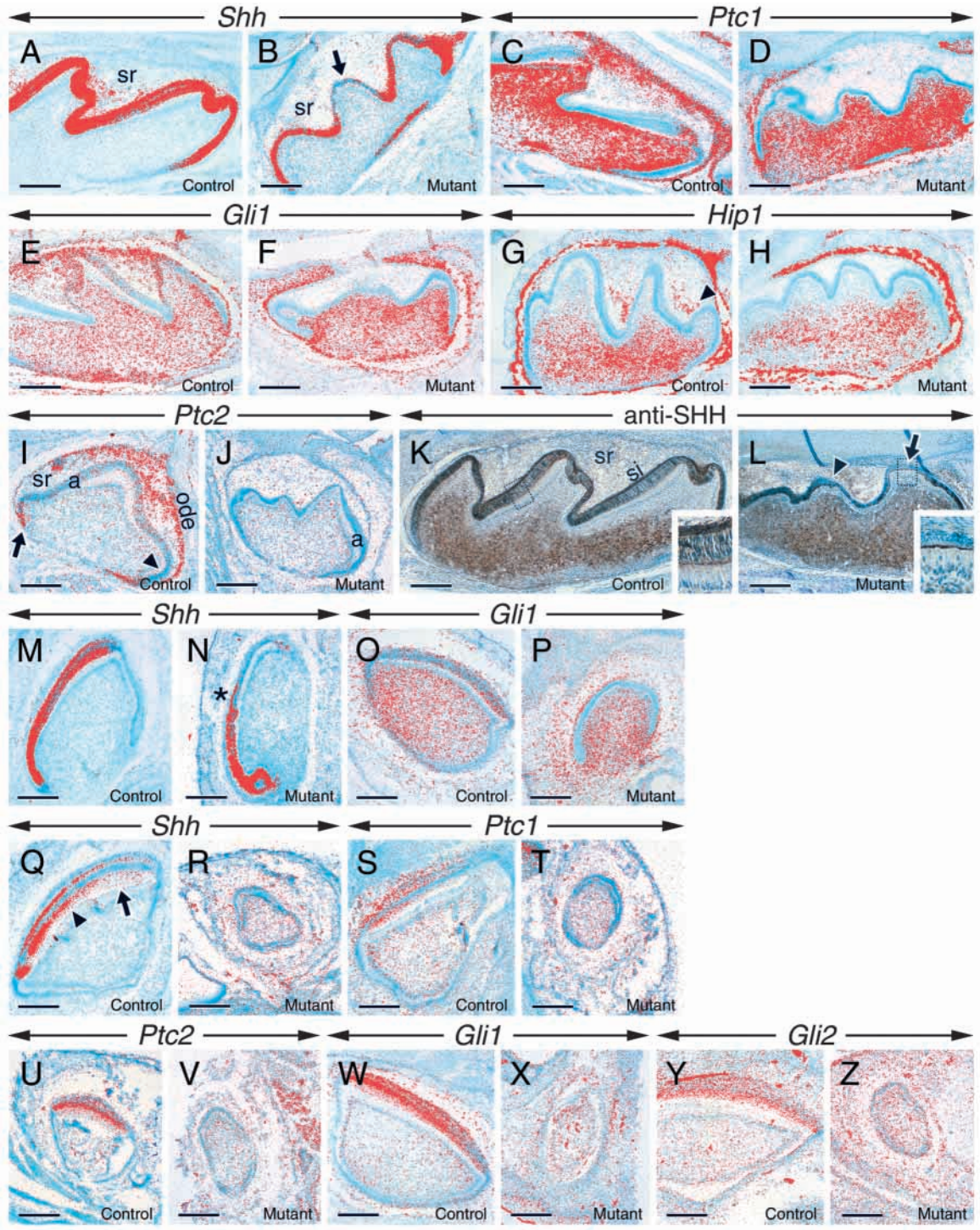

present in the dental papilla, preodontoblasts and polarizing odontoblasts (Fig. 6E,I and data not shown). Thereafter, *amelin* mRNA and protein appeared in differentiating ameloblasts and was strongly increased and maintained in ameloblasts (Fig. 6K and data not shown). In contrast, in mutant molars and incisors, *amelin* transcripts and protein were already detected in preameloblasts that were adjacent to either preodontoblasts or polarizing odontoblasts, prior to predentin secretion (Fig. 6F,J and data not shown), and remained strong at later stages (Fig. 6L and data not shown). Immunohistochemistry with anti-calbindin D28K antibody showed staining in preameloblasts that are either adjacent to polarized odontoblasts or a thin layer of predentin (Fig. 6G), whereas in *Smo* mutants molars calbindin staining was present at a developmentally earlier stage, in preameloblasts adjacent either to preodontoblasts or polarized odontoblasts (Fig. 6H). These data suggest that mutant ameloblasts 'mature' precociously and express genetic markers of post-mitotic ameloblasts, without undergoing the cytological changes characteristic of the ameloblast proper.

Fig. 5. *Shh* expression and *Shh* responsiveness during late tooth development in *Smo* mutants. Section through control (A,C,E,G,I,K,M,O, Q,S,U,W,Y) and *Smo* mutant (B,D,F,H,J,L,N,P,R,T,V,X,Z) teeth at 1 dpp. In situ hybridizations for *Shh* (A,B,M,N,Q,R); *Ptc1* (C,D,S,T); *Gli1* (E,F,O,P,W,X); *Hip1* (G,H); *Ptc2* (I,J,U,V); *Gli2* (Y,Z). Immunohistochemistry with Ab80 showing SHH protein distribution (K,L). Parasagittal (A-H,K,L) and frontal (I,J) sections through the molar region. Frontal sections at the middle (M-P) and anterior (Q-Z) segments of incisors. *Shh* expression is dramatically decreased in mutant ameloblasts facing predentin (arrow in B). The stratum intermedium continues to express Shh for only a short period before expression is severely decreased (asterisk in N). The signal in the stellate reticulum (SR, arrowhead in G) is artefactual and is due to refractile properties of displaced red blood cells and not to silver grains in SR cells. In I, the arrow points to the inner dental epithelium at the cervical loop and the arrowhead shows preameloblasts. In L, the arrowhead indicates preameloblasts adjacent to polarized odontoblasts and the arrow, preameloblasts adjacent to predentin matrix. In the mutant molar (L), Shh protein has accumulated in large amounts in the predentin facing preameloblasts, which show low amounts of Shh staining. This is probably due to minute amounts of Shh protein, emanating from preameloblasts and possibly also from the SI, which become trapped within predentin matrix, as these mutant cells express extremely low levels of *Ptc2* and *Ptc1* and thus may be unable to sequester Shh protein. The insets in K and L show high magnifications of the boxed areas. In Q, the arrowhead points to polarizing ameloblasts and the arrow to presecretory ameloblasts. a, ameloblasts; ode, outer dental epithelium; si, stratum intermedium; sr, stellate reticulum. Scale bars: 200 μm.

Smo ablation leads to down-regulation of transcripts for *DSP* and *Dlx7* in ameloblasts without affecting other genetic markers in odontoblasts and presecretory ameloblasts

As Shh signaling appears to be intact in the dental mesenchyme and its derivatives, we expected that these would not be affected in *Smo* mutants. However, the altered differentiation and responsiveness of ameloblasts in *Smo* mutants might have indirectly affected mesenchymal components. To address this issue, we examined the expression of a number of genetic markers, that are known to be initiated or upregulated upon ameloblast or odontoblast differentiation, including *PDGFRα*,

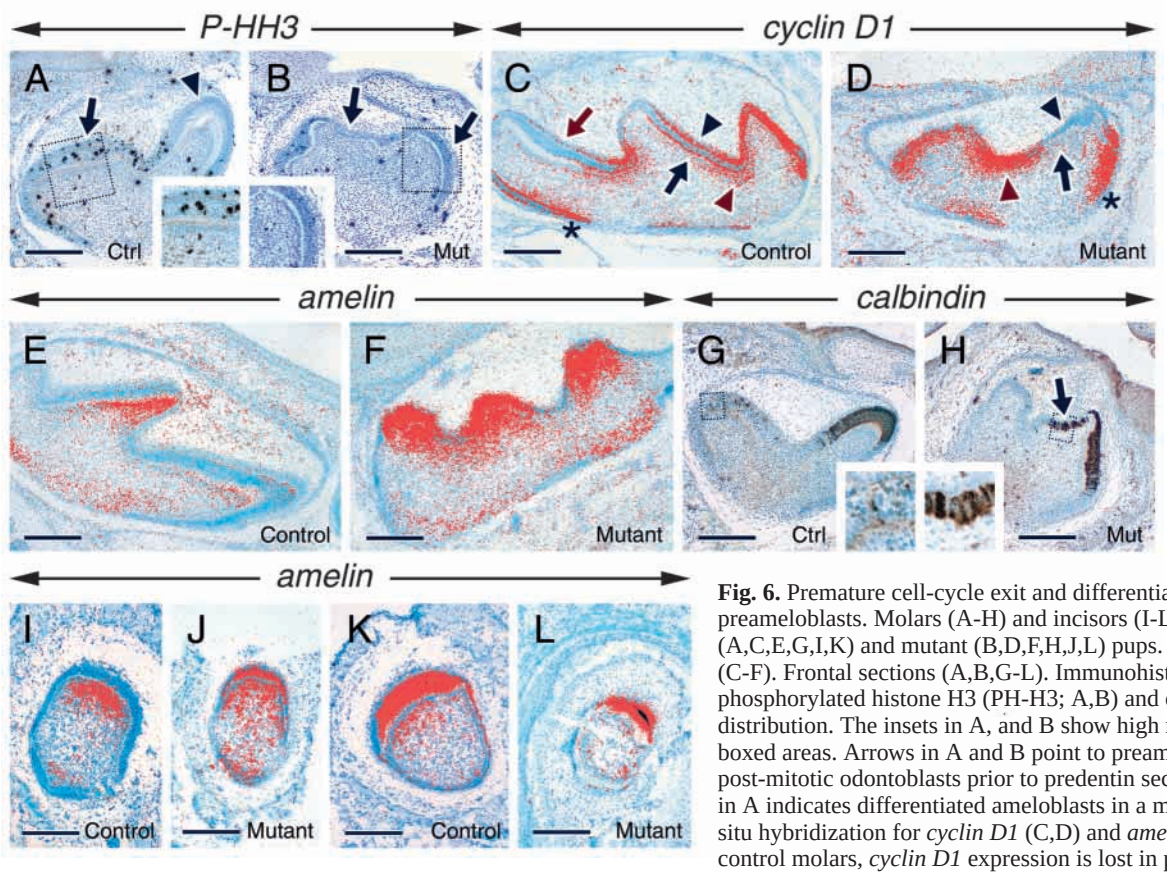

Fig. 6. Premature cell-cycle exit and differentiation of *Smo* mutant preameloblasts. Molars (A-H) and incisors (I-L) from control (A,C,E,G,I,K) and mutant (B,D,F,H,J,L) pups. Parasagittal sections (C-F). Frontal sections (A,B,G-L). Immunohistochemistry showing phosphorylated histone H3 (PH-H3; A,B) and calbindin D28K (G,H) distribution. The insets in A, and B show high magnifications of the boxed areas. Arrows in A and B point to preameloblasts adjacent to post-mitotic odontoblasts prior to predentin secretion. The arrowhead in A indicates differentiated ameloblasts in a more mature cusp. In situ hybridization for *cyclin D1* (C,D) and *amelin* (E,F,I-L). In control molars, *cyclin D1* expression is lost in post-mitotic ameloblasts facing the first layer of predentin matrix in the most advanced cusp (red arrow in C), whereas preameloblasts and the overlying stratum intermedium (black arrowhead in C) facing post-mitotic odontoblasts (black arrow in C) continue to express *cyclin D1*. *cyclin D1* expression is prematurely lost in *Smo* mutant preameloblasts and stratum intermedium (black arrowhead in D) adjacent to post-mitotic odontoblasts (arrow in D) prior to predentin secretion. Asterisks in C and D show proliferating cells at the cervical loops and red arrowheads show preodontoblasts. In D the section is through the less-developed cusps of the first molar region. In control molars (E), at the level of the less mature cusps, *amelin* is expressed in polarizing odontoblasts and is barely detectable in preameloblasts adjacent to them. In the *Smo* mutant molars (F), *amelin* is expressed prematurely at high amounts in preameloblasts facing polarizing odontoblasts in several cusps. Note that the cusps in the molar in F are at the same developmental stage as the left cusp of the molar in E. Arrow in H indicates preameloblasts adjacent to preodontoblasts. The insets in G and H show high magnifications of the boxed areas. Sections through the middle segment of the incisors showing absence of *amelin* expression in control preameloblasts (I) and premature expression by mutant preameloblasts (J). Sections through the anterior segment of incisors (K,L) showing *amelin* expression by ameloblasts. Scale bars: 200 μm (A-L).

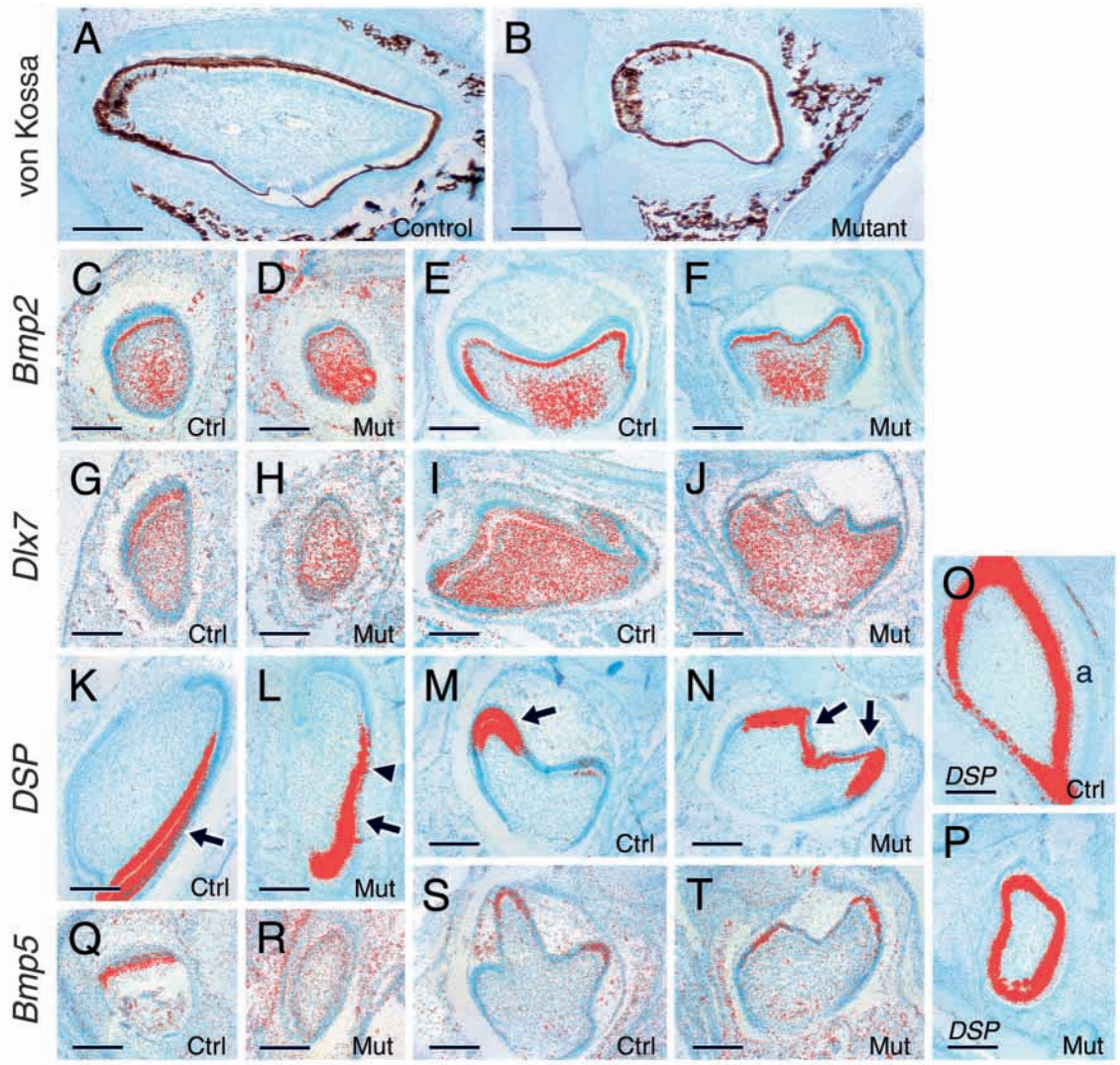

Fig. 7. Normal differentiation of odontoblasts and altered differentiation of ameloblasts in *Smo* mutant teeth. Parasagittal (A,B,K,L,O,P) and frontal (C-J,M,N,Q-T) sections at 1 dpp. Sections from control (ctrl; A,C,E,G,I,K,M,O,Q,S) and mutant (mut, B,D,F,H,J,L,N,P,R,T) teeth. von Kossa staining of mineralized dentin matrix (A,B). In situ hybridization for *Bmp2* (C-F), *Dlx7* (G-J), *DSP* (K-P) and *Bmp5* (Q-T). *Bmp2* and *DSP* are expressed normally in odontoblasts in *Smo* mutant teeth (C-F,K-P). *Dlx7* expression is severely decreased in mutant ameloblasts (G-J). *DSP* is expressed in preameloblasts facing predentin matrix (arrows in K and M) and is downregulated in secretory ameloblasts (a in O) in control teeth. In mutants, *DSP* expression is severely decreased in preameloblasts facing predentin matrix (arrows in L and N). The arrowhead in L indicates the start of decline of *DSP* expression in preameloblasts. *Bmp5* is expressed in secretory ameloblasts (Q) and in differentiating ameloblasts (S) in control teeth. At the anterior segment of mutant incisors, *Bmp5* expression is severely decreased in ameloblasts (R) but is normal in the less-mature ameloblasts in molars (T). Signals outside the tooth are sometimes due to refractile structures such as erythrocytes, cellular fragments or tissue folding. Scale bar: 200 μm.

DSP, *DMP1*, *Dlx3*, *Dlx7*, *Msx2*, *Bmp2*, *Bmp4*, *Bmp5*, and *Bmp7* (Fig. 7 and data not shown).

Odontoblasts differentiated normally on schedule and secreted normal predentin/dentin matrix in *Smo* mutant teeth. This is supported by the presence of normally polarized odontoblasts and normal mineralization of dentin matrix, as shown by von Kossa staining (Fig. 7A,B) and odontoblast expression of *PDGFRα*, *DMP1*, *Bmp2*, *Dlx7 and DSP* (Fig. 7C-P and data not shown). In contrast, cells of the ameloblastic lineage showed temporospatial alterations of the expressions of *Dlx7*, *DSP*, *Bmp4*, *Bmp5* and *Bmp7*. In *Smo* mutant incisors and molars, expression of *Dlx7* in differentiating ameloblasts was considerably less than in controls (Fig. 7G-J). These data suggest a possible regulation of *Dlx7* by Shh during ameloblast differentiation. It is noteworthy that in the dental epithelium of incisors, *Dlx7* expression is confined to the amelogenic labial epithelium (Fig. 7G). As shown in control incisors and molars, in addition to its expression in odontoblasts, *DSP* is known to be transiently expressed in preameloblasts adjacent to the first layer of predentin (Fig. 7K,M) and then lost in secretory ameloblasts (Fig. 7O). However, in *Smo* mutant incisors and molars (Fig. 7L,N) *DSP* transcripts were lost precociously from ameloblasts (Fig. 7L,N). This was not secondary to cell death in mutant ameloblasts, as these cells continued to express

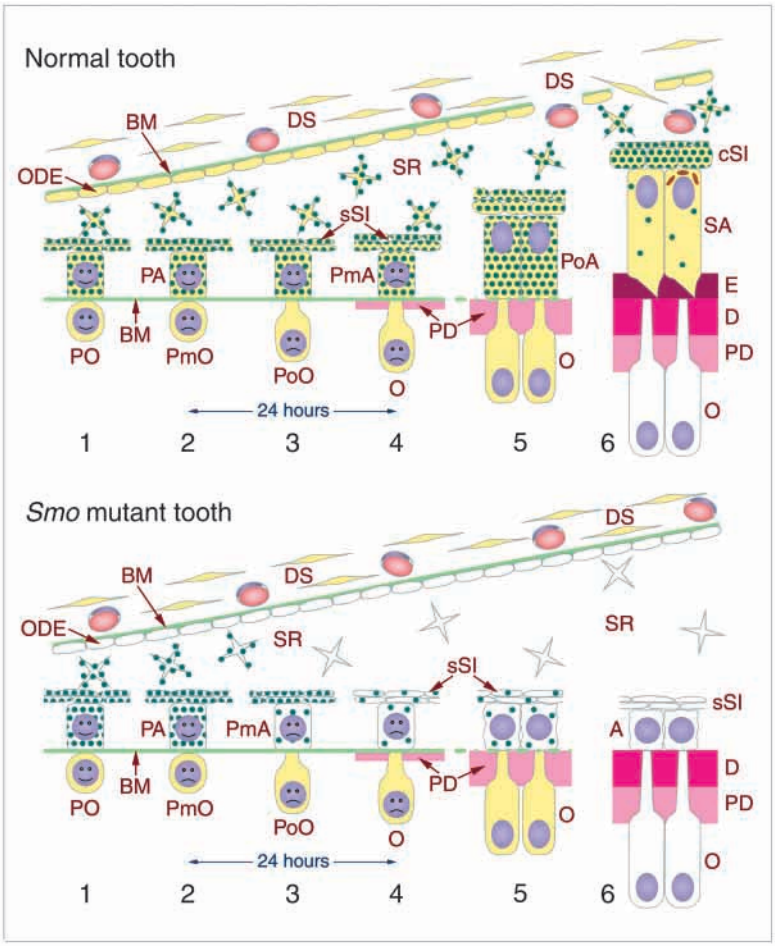

Fig. 8. Schematic drawing showing Shh expression (stippled green) and responsiveness (yellow) as well as the cytological changes occuring in the enamel organ and odontoblast layer during the gradual differentiation process in a normal (upper panel) and in a *Smo* mutant (lower panel) tooth. Proliferating cells are represented by smiling nuclei and post-mitotic cells are represented by non-smiling or plain nuclei. In a normal tooth, at stage 4, preameloblasts facing the first layer of predentin matrix (PD, pink) withdraw from the cell cycle and become post-mitotic (PmA). This occurs about 24 hours after the adjacent odontoblasts become postmitotic (stage 2), polarize (stage 3) and secrete PD (stage 4). Polarizing ameloblasts (PoA) continue to grow, they attain their full size at stage 6 and become secretory ameloblasts (SA) displaying Tomes' processes and secrete enamel matrix (E, dark red). Cells of the stratum intermedium overlying PoA and SA increase in size and become cuboidal (cSI). Shortly before enamel secretion, gaps appear in the outer dental epithelium (ODE) and blood vessels and fibroblasts from the dental sac (DS) start to invade the stellate reticulum (SR). Shh is produced in large amounts in proliferating preameloblasts (PA), PmA, PoA, squamous stratum intermedium (sSI) and cSI. *Shh* expression and Shh synthesis decline thereafter in presecretory ameloblasts (not represented) and SA (stage 6). In the normal tooth, both the enamel organ and dental mesenchyme are responsive to Shh signaling. In the *Smo* mutant tooth, Shh responsiveness, cell proliferation, growth and differentiation are preserved in the dental mesenchyme, including the dental papilla (not represented), dental sac and the odontoblast layer. However, Shh responsiveness is absent in the enamel organ at all stages (stages 1-6). Mutant preameloblasts become post-mitotic prematurely (stage 3) before predentin secretion by the adjacent odontoblasts. Mutant ameloblasts fail to grow in size, are unpolarized and unable to produce enamel matrix. The mutant stratum intermedium cells remain small and squamous. The outer dental epithelium layer remains continuous, and the stellate reticulum remains avascular. In addition, a premature gradual decrease of Shh production occurs in the mutant ameloblasts, stratum intermedium and stellate reticulum. A, ameloblast; BM, basement membrane (light green); D, dentin (dark pink); O, odontoblast; PmO, post-mitotic odontoblast; PO, proliferating preodontoblast; PoO, polarizing odontoblast.

other late genetic markers, such as *Msx2* and *amelin* (see Fig. 6P and data not shown) at very high levels in the anterior portion of the incisor. These data provide further evidence for the premature differentiation of *Smo* mutant ameloblasts. Finally, while in control incisors, *Bmp4*, *Bmp5* and *Bmp7* (Fig. 7Q and data not shown) were expressed in secretory ameloblasts, expressions of these genes were severely down-regulated in mutant ameloblasts (Fig. 7R and data not shown). However, at an earlier stage in both incisors and molars from *Smo* mutants, preameloblasts and ameloblasts expressed *Bmp4* and *Bmp5* as in controls (Fig. 7S,T and data not shown).

DISCUSSION

We have shown previously (Dassule et al., 2000) that conditional removal of Shh activity from the dental epithelium, the sole tooth compartment responsible for Shh production, alters growth, morphogenesis and cytological organization in both the dental epithelium and mesenchyme. By the conditional ablation of *Smo* within the dental epithelium, we now provide evidence that Shh signaling within the EEO itself is crucial for the normal control of cell proliferation, cell differentiation, cell growth and cell polarity, and consequently for appropriate morphogenesis of the tooth (summarized schematically in Fig. 8).

Epithelial Shh signaling regulates cell proliferation and cell differentiation in epithelial compartments of the tooth

Loss of Smo activity in the dental epithelium led to the expected abrogation of Shh responsiveness within the EEO, whereas Shh signaling was maintained in the dental mesenchyme, which developed normally at all stages up to 1 dpp. *Smo* mutant molars were fused and displayed alterations in cusp morphogenesis. In *Smo* mutant teeth, preameloblasts and cells of the SI withdrew from the cell cycle prior to predentin secretion, as evidenced by loss of *cyclin D1* mRNA and PH-H3 protein, and exhibited molecular features of more mature cells. These data suggest a direct requirement for Shh activity in regulating proliferation within the dental epithelium. Rather than exiting the cell-cycle coincident with secretion of

the first layer of predentin matrix (Ruch, 1987; Ruch, 1990), in the absence of Shh signal transduction, preameloblast and cells of the SI withdraw before matrix accumulation. Thus, Shh may exert a direct mitogenic effect on these cells, at least in part, by promoting *cyclin D1* transcription to control the G_1/S transition. After exiting the cell cycle, preameloblasts underwent premature differentiation. Thus, maintaining these cells in a proliferative state may be one mechanism by which the pace and position of ameloblast differentiation is controlled in the IEE. Alternatively, Shh may regulate cell proliferation and cell differentiation independently. In this regard it is noteworthy that a second member of this family, Ihh, coordinates proliferation and differentiation of chondrocytes by distinct mechanisms during morphogenesis of the endochondral skeleton (reviewed by McMahon et al., 2002).

A key role of hedgehog members as mitogens has been shown in several developmental settings (for a review, see McMahon et al., 2002). A direct hedgehog input controlling cell proliferation has been best characterized in the cerebellum (Dahmane and Ruiz i Altaba, 1999; Wallace, 1999; Wechsler-Reya and Scott, 1999; Kenney and Rowitch, 2000) and cartilage (Long et al., 2001), as well as in the optic lamina and eye in *Drosophila* (Huang and Kunes, 1996; Huang and Kunes, 1998; Duman-Scheel et al., 2002). Recent evidence indicates that hedgehog proteins are likely to exert their mitogenic activity through regulation of G_1 and G_1/S cyclins. In the cerebellum, Shh stimulates granule cell progenitor (GCP) proliferation by promoting D-type cyclins (Kenney and Rowitch, 2000). In the developing cartilage, Ihh's mitogenic activity also promotes *cyclin D1* transcription (Long et al., 2001). Finally, recent studies in *Drosophila* established a link between hedgehog and D-type and E-type cyclins in controlling cell proliferation and growth (Duman-Scheel et al., 2002). Together, these data indicate that transcriptional induction of D-type cyclins is a likely common and conserved mechanism by which hedgehog proteins promote cell proliferation. In addition, studies in transfected cells have shown that Shh ligand disrupts an interaction between Ptc1 and cyclin B1 at the G_2/M transition, thereby allowing the activation of M-phase-promoting factor and cell cycle progression (Barnes et al., 2001). It would be of interest to determine whether these events also occur in normal cells that are responsive to Shh.

During the late bell stage, both the proliferating preameloblasts and the cells of the SI strongly express *Shh*, and both respond to Shh signaling as judged by expression of key targets such as *Ptc1* and *Gli1*. Whether Shh operates in an autocrine or paracrine manner within and between these cell layers, respectively, is unclear at present. One possible way to examine this issue would be by removal of Shh activity specifically from the SI.

What makes preameloblasts exit the cell cycle? Our analyses show that both the proliferating preameloblasts and the newly differentiated ameloblasts both express high levels of Shh and are Shh responsive. This raises the question of what normally triggers exit from the cell cycle in ameloblasts. The same situation is found in the developing cerebellum, where GCPs migrate towards Purkinje neurons, the source of Shh, and thus become exposed to higher concentrations of the protein. However, GCPs stop dividing by the time they reach the internal part of the external germinal layer, although they remain highly responsive to Shh. It is unlikely that termination of preameloblast proliferation is due to reduced exposure or responsiveness to Shh. This may be the result of conversion of a proliferative response into a differentiative one or to the activation of antagonizing signals.

Smo mutant first and second molars were fused and developed into a single anlage. It is noteworthy that molar fusions can occur in both animals and humans (Sofaer and Shaw, 1971; Turell and Zmener, 1999), but their etiology is unknown. In addition, *Smo* mutant molars had abnormally shaped, small and shallow cusps. Signaling from the enamel knots has been shown to pattern cuspidogenesis in molars (Thesleff et al., 2001). In *Smo* mutants molars, the primary and secondary enamels knots developed normally and expressed several genetic markers of these structures. We therefore propose that cusp dysmorphogenesis in *Smo* mutant molars may be secondary to the alterations in cell proliferation profiles within the EEO.

Shh as a modulator of epithelial-epithelial interactions necessary for ameloblast and SI cytodifferentiation

Smo mutant ameloblasts failed to assume the morphological features of differentiating cells, and the SI remained squamous in nature. At this developmental stage in *Smo* mutant teeth, odontoblasts developed and differentiated normally, and predentin/dentin matrices were secreted on schedule. These data indicate that Shh activity within the dental epithelium is necessary for proper cytodifferentiation of preameloblasts and cells of the SI.

In the mouse incisor, *Shh* and *Dlx7* were expressed exclusively in the labial amelogenic epithelium, and *Dlx7* expression was down-regulated in *Smo* mutant teeth. Transcripts for *Ptc2* and *Gli1* showed a polarized localization at the basal and perinuclear pole of polarizing ameloblasts, which is adjacent to the SI.

The events leading to ameloblast cytodifferentiation are not clear. Early tissue recombination studies using dental and non-dental tissues have shown that ameloblast cytodifferentiation requires functional odontoblasts (Kollar and Baird, 1970; Ruch et al., 1973), and that acellular dental matrices can promote ameloblast cytodifferentiation as well (Karcher-Djuricic et al., 1985). In those studies (and J. V. Ruch, personal communication), the development of an EEO (and not only a monolayer of IDE) from non-dental and dental epithelia was shown to be a prerequisite for induction of ameloblast cytodifferentiation by the mesenchymal components. Thus, there is additional need for an epithelial endogenous control, possibly involving interactions between the SI and preameloblasts. However, the different developmental fates of the labial amelogenic and lingual non-amelogenic IDE of the incisor have been shown to be governed by an endogenous epithelial regulation, independent of odontoblasts/predentin/dentin (Amar et al., 1986; Amar et al., 1989; Ruch, 1990). The role of the SI is unknown. This cell layer has been suggested to play a role in ameloblast differentiation based on morphological differences in the relationships between ameloblasts and the SI in the amelogenic zones as compared to the non-amelogenic zones of rodent teeth (Wakita and Hinrichsen, 1980; Nakamura et al., 1991). The SI has also been suggested to give rise to cells of the SR (Hunt and Paynter,

1963). The polarized Shh responsiveness in ameloblasts suggests that Shh emanating from the SI may play a role in ameloblast cytodifferentiation. However, Shh is expressed in both the SI and the differentiating ameloblasts.

Together, these data suggest that although the dental mesenchyme is necessary for ameloblast cytodifferentiation, it is not sufficient, and autocrine and/or paracrine epithelial-epithelial interactions within the EEO play an important role. Thus, our *Smo* conditional allele provides a molecular basis for understanding the early experimental studies, and suggests that Shh may be an endogenous epithelial factor regulating ameloblast cytodifferentiation. The asymmetrical expression of *Shh* and *Dlx7* in the incisor and the downregulation of *Dlx7* expression in mutant ameloblasts raise the question of whether Shh is, indeed, involved in the determination of the different developmental fates between the labial and lingual dental epithelia through the regulation of *Dlx7* expression.

Shh regulates growth and polarization of epithelial dental cells

The preameloblast is a unique epithelial cell, as upon differentiation into a secretory ameloblast it reverses its polarity: the pole of the cell that was originally basal (towards the basement membrane) becomes structurally and functionally apical (Frank and Nalbandian, 1967). In addition, differentiation of the ameloblast is accompanied by a significant increase in size and by an extensive development of cytoplamic organelles (Frank and Nalbandian, 1967). At this time, cells of the SI also increase in size (Wakita and Hinrichsen, 1980).

At the differentiation stage, despite the presence of predentin/dentin matrices, *Smo* mutant ameloblasts and cells of the SI failed to grow in size, remained unpolarized, and were characterized by a paucity of organelles. In spite of this, mutant ameloblasts expressed several genetic markers of differentiated cells. As in polarizing ameloblasts, *Ptc2* and *Gli1* transcripts were enriched in the basal and perinuclear compartment of control presecretory and secretory ameloblasts. By this time, Shh production was barely detectable in these cells, whereas the overlying SI continued to produce Shh. These data suggest that ameloblast growth and polarization and the development of a cuboidal SI are Shh dependent. Hence, Shh may have anabolic activities regulating organelle and membrane biosynthesis. In addition, the phenotype of Smo mutant ameloblasts suggests that control of differentiation may be uncoupled from regulation of growth and polarization.

Smo mutant ameloblasts failed to show the typical polarized and localized distribution of E-cadherin and ZO-1 and lacked β-tubulin accumulation. Polarized epithelial cells interact with each other through specialized junctional complexes (Farquhar and Palade, 1963). Junctional complexes and microtubules are involved not only in maintaining epithelial cell polarity and partitioning the plasma membrane into apical and basolateral domains, but also in integrating mechanical and signaling pathways (Kirkpatrick and Peifer, 1995; Barth et al., 1997; Gundersen and Cook, 1999; Tsukita et al., 1999; Vasioukhin and Fuchs, 2001; Jamora and Fuchs, 2002). Previous TEM and immunological studies have shown that during the cytodifferentiation stage, numerous junctional complexes are established within the ameloblast and SI layers as well as between these two cell layers (Wakita and Hinrichsen, 1980; Fausser et al., 1998). Together, these data reveal roles for Shh signaling in controlling epithelial cell size and polarity.

The intracellular localization of *Ptc2* and *Gli1* transcripts to the basal and perinuclear compartments of presecretory and secretory ameloblasts is an intriguing finding. This suggests that signaling from the SI to ameloblasts may be linked to the polarized distribution of these RNAs, potentially providing an efficient mechanism for the targeting of their protein products to the appropriate subcellular compartments. Epithelial polarity is established and maintained through specific subcellular trafficking of proteins to different subcellular compartments or membranes (Ikonen and Simons, 1998; Mostov et al., 2000). Protein trafficking and cell polarity involve not only the directed movement of specialized vesicles after protein synthesis (Ikonen and Simons, 1998), but also occur via the subcellular localization of transcripts (RNA sorting) prior to translation (Palacios and St. Johnston, 2001). Why *Ptc2* and *Gli1* transcripts show this distribution in the ameloblast cytoplasm, but *Ptc1* and *Gli2* transcripts do not, is not clear.

In conclusion, the expression patterns of Shh signaling components and the tooth phenotype of *Smo* mutant mice provide evidence for the presence of subtle and yet exquisite Shh signaling within the dental epithelium. Tooth development is orchestrated by Shh-dependent epithelial-mesenchymal and epithelial-epithelial interactions.

We are grateful to Drs C. Betsholtz, H. Edlund, A. George, D. Kingsley, U. Lendahl, M. MacDougall, E. Robertson, P. Sharpe, I. Thesleff, K. Weiss, J. Wozney and T. Wurtz for probes and antisera. We also thank Drs I. Thesleff and J. V. Ruch for advice and kindness. We wish to express our gratitude to T. Chadashvili and J. McMahon for mouse genotyping, H. Dassule for initially setting up mouse crosses, P. Cassidy for efficiency and kindness and to K. Hallberg for generously linearizing some of the plasmids. This work was supported by the Swedish Research Council (Grants 2789 and 14100) and the County Council of Västra Götaland to A. G. L. and A. L.; and by grants from the NIH to M. B. (K22DE14230), A. P. M. (NS 33642) and R. M. (DE 11697).

REFERENCES

Åberg, T., Wozney, J. and Thesleff, I. (1997). Expression patterns of Bone Morphogenetic Proteins (Bmps) in the developing mouse tooth suggest roles in morphogenesis and differentiation. *Dev. Dyn.* **210**, 383-396.

Amar, S., Karcher-Djuricic, V., Meyer, J. M. and Ruch, J. V. (1986). The lingual (root-analogue) and the labial (crown analogue) mouse incisor dentin promotes ameloblast differentiation. *Arch. Anat. Microsc. Morphol. Exp.* **75**, 229-239.

Amar, S., Luo, W., Snead, M. L. and Ruch, J. V. (1989). Amelogenin gene expression in mouse incisor heterotypic recombinations. *Differentiation* **41**, 56-61.

Barnes, E. A., Kong, M., Ollendorff, V. and Donoghue, D. J. (2001). Patched1 interacts with cyclin B1 to regulate cell cycle progression. *EMBO J.* **20**, 2214-2223.

Barth, A. I., Nathke, I. S. and Nelson, W. J. (1997). Cadherins, catenins and APC protein: interplay between cytoskeletal complexes and signaling pathways. *Curr. Opin. Cell Biol.* **9**, 683-690.

Bitgood, M. J. and McMahon, A. P. (1995). Hedgehog and Bmp genes are coexpressed at many diverse sites of cell-cell interaction in the mouse embryo. *Dev. Biol.* **172**, 126-138.

Boström, H., Willetts, K., Pekny, M., Leveén, P., Lindahl, P., Hedstrand, H., Pekna, M., Hellström, M., Gebre-Medhin, S., Schalling, M., Nilsson, M., Kurland, S., Törnell, J., Heath, J. K. and Betsholtz, C. (1996). PDGF-A signaling is a critical event in lung alveolar myofibroblast development and alveogenesis. *Cell* **85**, 863-873.

Bumcrot, D. A., Takada, R. and McMahon, A. P. (1995). Proteolytic processing yields two secreted forms of sonic hedgehog. *Mol. Cell. Biol.* **15**, 2294-2303.

Carpenter, D., Stone, D. M., Bruch, J., Armanini, M., Frantz, G., Rosenthal., A. and de Sauvage, F. (1998). Characterization of two patched receptors for the vertebrate hedgehog family. *Proc. Natl. Acad. Sci. USA* **95**, 13630-13634.

Cerny, R., Slaby, I., Hammarström, L. and Wurtz, T. (1996). A novel gene expressed in rat ameloblasts codes for proteins with cell binding domains. *J. Bone Miner. Res*. **11**, 883-891.

Cohn, S. A. (1957). Development of the molar teeth in the albino mouse. *Am. J. Anat*. **101**, 295-320.

Dahmane, N. and Ruiz i Altaba, A. (1999). Sonic hedgehog regulates the growth and patterning of the cerebellum. *Development* **126**, 3089-3100.

Dassule, H. R., Lewis, P., Bei, M., Maas, R. and McMahon, A. P. (2000). Sonic Hedgehog regulates growth and morphogenesis of the tooth. *Development* **127**, 4775-4785.

Duman-Scheel, M., Weng, L. and Du, W. (2002). Hedgehog regulates cell growth and proliferation by inducing cyclin D and cyclin E. *Nature* **417**, 299-304.

Elms, T. N. and Taylor, A. N. (1987). Calbindin-D28K localization in rat molars during odontogenesis. *J. Dent. Res.* **66**, 1431-1434.

Farquhar, M. G. and Palade, G. E. (1963). Junctional complexes in various epithelia. *J. Cell Biol*. **17**, 375-412.

Fausser, J. L., Schlepp, O., Aberdam, D., Meneguzzi, G., Ruch, J. V. and Lesot, H. (1998). Localization of antigens associated with adherens junctions, desmosomes, and hemidesmosomes during murine molar morphogenesis. *Differentiation* **63**, 1-11.

Fong, C. D., Cerny, R., Hammarström, L. and Slaby, I. (1998). Sequential expression of an amelin gene in mesenchymal and epithelial cells during odontogenesis. *Eur. J. Oral Sci.* **106**, 324-330.

Frank, R. M. and Nalbandian, J. (1967). Ultrastructure of amelogenesis. In *Structural and Chemical Organization of Teeth, vol I* (ed. A. E. W. Miles), pp. 399-466. New York: Academic Press.

Frank, R. M. and Nalbandian, J. (1989). Development of dentine and pulp. In *Handbook of Microscopic Anatomy. Vol V/6: Teeth* (ed. A. Oksche and L. Vollrath), pp. 73-171. Heidelberg: Springer-Verlag.

Gaunt, J. (1956). The development of enamel and dentin on the molars of the mouse with an account to the enamel-free areas. *Acta Anat.* **28**, 111-134.

Gritli-Linde, A., Lewis, P., McMahon, A. P. and Linde, A. (2001). The whereabouts of a morphogen: Direct evidence for short- and long-range activity of Hedgehog signaling peptides. *Dev. Biol*. **236**, 364-386.

Gundersen, G. G. and Cook, T. (1999). Microtubules and signal transduction. *Curr. Opin. Cell Biol.* **11**, 81-94.

Harada, H., Kettunen, P., Jung, H.-S., Mustonen, T., Wang, Y. A. and Thesleff, I. (1999). Localization of putative stem cells in dental epithelium and their association with Notch and FGF signaling. *J. Cell Biol*. **147**, 105-120.

Hardcastle, Z., Mo, R., Hui, C.-C. and Sharpe, P. (1998). The Shh signaling pathway in tooth development: defects in *Gli2* and *Gli3* mutants. *Development* **125**, 2803-2811.

Hay, M. (1961). The development in vivo and in vitro of the lower incisor and molar of the mouse. *Arch. Oral Biol*. **3**, 86-109.

Huang, Z. and Kunes, S. (1996). Hedgehog, transmitted along retinal axons, triggers neurogenesis in the developing visual centers of the Drosophila brain. *Cell* **86**, 411-422.

Huang, Z. and Kunes, S. (1998). Signals transmitted along retinal axons in *Drosophila*: Hedgehog signal reception and the cell circuity of lamina cartridge assembly. *Development* **125**, 3753-3764.

Hunt, A. M. and Paynter, K. J. (1963). The role of the stratum intermedium in the development of the guinea pig molar. A study of cell differentiation and migration using tritiated thymidine. *Arch. Oral Biol.* **8**, 64-73.

Ikonen, E. and Simons, K. (1998). Protein and lipid sorting from the trans-Golgi network to the plasma membrane in polarized cells. *Sem. Cell Dev. Biol*. **9**, 503-509.

Ingham, P. W. and McMahon, A. P. (2001). Hedgehog signaling in animal development: paradigms and principles. *Genes Dev*. **15**, 3059-3087.

Jamora, C. and Fuchs, E. (2002). Intercellular adhesion, signaling and the cytoskeleton. *Nat. Cell Biol*. **4**, 101-108.

Jernvall, J., Åberg, T., Kettunen, P., Keränen, S. and Thesleff, I. (1998). The life history of an embryonic signaling center: BMP-4 induces p21 and is associated with apoptosis in the mouse tooth enamel knot. *Development* **125**, 161-169.

Jernvall, J. and Thesleff, I. (2000). Reiterative signaling and patterning in mammalian tooth morphogenesis. *Mech. Dev*. **92**, 19-29.

Karcher-Djuricic, V., Staubli, A., Meyer, J. M. and Ruch, J. V. (1985). Acellular dental matrices promote functional differentiation of ameloblasts. *Differentiation* **29**, 169-175.

Kenney, A. M. and Rowitch, D. H. (2000). Sonic hedgehog promotes G(1) cyclin expression and sustained cell cycle progression in mammalian neuronal precursors. *Mol. Cell. Biol*. **20**, 9055-9067.

Kirkpatrick, C. and Peifer, M. (1995). Not just glue: cell-cell junctions as cellular signaling centers. *Curr. Opin. Genet. Dev*. **5**, 56-65.

Kollar, E. J. and Baird, G. (1970). Tissue interactions in embryonic mouse tooth germs. II. The inductive role of the dental papilla. *J. Embryol. Exp. Morphol*. **24**, 173-186.

Lefkowitz, W., Bodecker, C. F. and Mardfin, D. F. (1953). Odontogenesis of the rat molar. *J. Dent. Res.* **32**, 749-762.

Lesot, H., Meyer, J. M., Ruch, J. V., Weber, K. and Osborn, M. (1982). Immunofluorescent localization of vimentin, prekeratin and actin during odontoblast and ameloblast differentiation. *Differentiation* **20**, 133-137.

Long, F., Zhang, X. M., Karp, S., Yang, Y. and McMahon, A. P. (2001). Genetic manipulation of hedgehog signaling in the endochondral skeleton reveals a direct role in the regulation of chondrocyte proliferation. *Development* **128**, 5099-5108.

Marti, E., Takada, R., Bumcrot, D. A., Sasaki, H. and McMahon, A. P. (1995). Distribution of Shh peptides in the developing chick and mouse embryo. *Development* **121**, 2537-2547.

McMahon, A. P., Ingham, P. W. and Tabin, C. (2002). The developmental roles and clinical significance of hedgehog signaling. *Curr. Topics Dev. Biol*. (in press).

Mostov, K. E., Verges, M. and Altschuler, Y. (2000). Membrane traffic in polarized epithelial cells. *Curr. Opin. Cell Biol*. **12**, 483-490.

Motoyama, J., Takabatake, T., Takeshima, K. and Hui, C. C. (1998). Ptch2, a second mouse patched gene is co-expressed with sonic hedgehog. *Nat. Genet*. **18**, 104-106.

Nakamura, M., Bringas, P. and Slavkin, H. C. (1991). Inner enamel epithelia synthesize and secrete enamel proteins during mouse molar occlusal "enamel-free area" development. *J. Craniofac. Genet. Dev. Biol*. **11**, 96-104.

Palacios, I. M. and St. Johnston, D. (2001). Getting the message across: The intracellular localization of mRNAs in higher eukaryotes. *Annu. Rev. Cell Dev. Biol*. **17**, 569-614.

Ruch, J. V., Karcher-Djuricic, V. and Gerber, R. (1973). Les déterminisms de la morphogenèse et des cytodifferenciations des ébauches dentaires de souris. *J. Biol. Buccale* **1**, 45-56.

Ruch, J. V. (1987). Determinism of odontogenesis. *Cell Biol. Rev*. **14**, 1-112.

Ruch, J. V. (1990). Patterned distribution of differentiating dental cells: facts and hypotheses. *J. Biol. Buccale* **18**, 91-98.

Slavkin, H. (1974). Embryonic tooth formation. A tool for developmental biology. *Oral Sci. Rev*. **4**, 7-136.

Slavkin, H. C. and Bringas, P. (1976). Epithelial-mesenchymal interactions during dentinogenesis. IV. Morphological evidence for direct heterotypic cell-cell contact. *Dev. Biol*. **50**, 428-442.

Smith, C. E. and Warshawsky, H. (1975). Cellular renewal in the enamel organ and the odontoblast layer of the rat incisor as followed by radioautography using 3H-thymidine. *Anat. Rec*. **183**, 523-562.

Sofaer, J. A. and Shaw, J. H. (1971). The genetics and development of fused and supernumerary molars in the rice rat. *J. Embryol. Exp. Morph*. **26**, 99-109.

Stevens, A., Lowe, J. and Bancroft, J. D. (1990). Bone. In *Theory and Practice of Histological Techniques* (ed. J. D. Bancroft and A. Stevens), pp. 309-341. New York: Churchill Livingstone.

Sun, D., Vanderburg, C. R., Odierna, G. S. and Hay, E. D. (1998). TGFβ3 promotes transformation of chicken palate medial edge epithelium to mesenchyme in vitro. *Development* **125**, 95-105.

Tabata, M. J., Matsumura, T., Liu, J. G., Wakisaka, S. and Kurisu, K. (1996). Expression of cytokeratin 14 in ameloblast-lineage cells of the developing tooth of rat, both in vivo and in vitro. *Arch. Oral Biol.* **41**, 1019-1027.

Thesleff, I., Barach, H. J., Foidart, J. M., Vaheri, A., Pratt, R. M. and Martin, G. R. (1981). Changes in the distribution of type IV collagen, laminin, proteoglycans, and fibronectin during mouse tooth development. *Dev. Biol.* **81**, 182-192.

Thesleff, I., Keränen, S. and Jernvall, J. (2001). Enamel knots as signaling centers linking tooth morphogenesis and odontoblast differentiation. *Adv. Dent. Res*. **15**, 14-18.

Thesleff, I. and Mikkola, M. (2002). The role of growth factors in tooth development. *Int. Rev. Cytol.* **217**, 93-135.

Tsukita, S., Furuse, M. and Itoh, M. (1999). Structural and signaling molecules come together at tight junctions. *Curr. Opin. Cell Biol*. **11**, 628-633.

Turell, I. L. and Zmener, O. (1999). Endodontic management of a mandibular third molar fused with a fourth molar. *Int. Endo. J*. **32**, 229-231.

Turksen, K., Kupper, T., Degenstein, L., Williams, I. and Fuchs, E. (1992). Interleukin 6: insights to its function in skin by overexpression in transgenic mice. *Proc. Natl. Acad. Sci. USA* **89**, 5068-5072.

Vaahtokari, A., Åberg, T., Jernvall, J., Keränen, S. and Thesleff, I. (1996). The enamel knot as a signaling center in the developing mouse tooth. *Mech. Dev*. **54**, 39-43.

Vasioukhin, V. and Fuchs, E. (2001). Actin dynamics and cell-cell adhesion in epithelia. *Curr. Opin. Cell Biol*. **13**, 76-84.

Wakita, M. and Hinrichsen, K. (1980). Ultrastructure of ameloblast-stratum intermedium border during ameloblast differentiation. *Acta Anat*. (Basel) **108**, 10-29.

Wallace, V. A. (1999). Purkinje-cell-derived Sonic hedgehog regulates granule neuron precursor cell proliferation in the developing mouse cerebellum. *Curr. Biol.* **9**, 445-448.

Warshawsky, H. (1968). The fine structure of secretory ameloblasts in rat incisor. *Anat. Rec*. **161**, 211-229.

Wechsler-Reya, R. J. and Scott, M. P. (1999). Control of neuronal precursor proliferation in the cerebellum by Sonic Hedgehog. *Neuron* **22**, 103-114.

Wilkinson, D. G., Bailes, J. A., Champion, J. E. and McMahon, A. P. (1987). A molecular analysis of mouse development from 8 to 10 days *post coitum* detects changes only in embryonic globin expression. *Development* **99**, 493-500.

Zhang, X. M., Ramalho-Santos, M. and McMahon, A. P. (2001). Smoothened mutants reveal redundant roles for Shh and Ihh signaling including regulation of L/R asymmetry by the mouse node. *Cell* **105**, 781-792.

Zhao, Z., Stock, D. W., Buchanan, A. and Weiss, K. (2000). Expression of Dlx genes during the development of the murine dentition. *Dev. Genes Evol.* **210**, 270-275.